Magnetization dynamics of Landau structures: tuning the response of mesoscopic magnetic objects using defects

2009 J. Phys.: Condens. Matter 21 436003

(http://iopscience.iop.org/0953-8984/21/43/436003)

J. Phys.: Condens. Matter **21** (2009) 436003 (7pp) doi:10.1088/0953-8984/21/43/436003

Magnetization dynamics of Landau structures: tuning the response of mesoscopic magnetic objects using defects

K Kuepper[1], S Wintz[2], J Raabe[3], M Buess[3], Ch Akhmadaliev[2], L Bischoff[2], C Quitmann[3] and J Fassbender[2]

[1] Institut für Festkörperphysik, University of Ulm, Albert-Einstein-Allee 11, D-89069 Ulm, Germany[4]
[2] Forschungszentrum Dresden-Rossendorf, PO Box 51 01 19, D-01314 Dresden, Germany
[3] Swiss Light Source, Paul Scherrer Institut, CH-5232 Villigen, Switzerland

E-mail: karsten.kuepper@uni-ulm.de and j.fassbender@fzd.de

Received 23 June 2009, in final form 17 August 2009
Published 8 October 2009
Online at stacks.iop.org/JPhysCM/21/436003

Abstract
Magnetic vortex cores are interacting with and can even be annihilated by artificial defects, such as holes. These defects have been fabricated by focused ion beam milling (FIB) into the magnetic domains, domain walls and the center of square-shaped vortices, known as Landau structures. We report the imaging of the magnetization dynamics of Landau structures containing holes by means of x-ray magnetic circular dichroism photo-emission electron microscopy (XMCD-PEEM). Due to the high lateral and temporal resolution of this method, the magnetic excitation spectrum, which is characteristic for the vortex–hole interaction, is investigated in detail. We find that the vortex core as well as domain walls can be trapped by small holes. With the help of micromagnetic simulations we show that the vortex gyrotropic motion frequency is enhanced, whereas the amplitude is significantly reduced in the case of non-centric holes in domain walls.

(Some figures in this article are in colour only in the electronic version)

1. Introduction

Ferromagnetic discs or square-shaped thin elements (of a few tens of nm thickness) with sub-micrometer lateral dimensions often comprise small cores of around 10–20 nm in size, with perpendicular magnetization. In the last few years these so-called magnetic vortices have attracted enormous attention [1–5]. The huge interest in magnetic vortices stems partly from the fact that a vortex can be understood as being a two-dimensional topological soliton, which are interesting due to a lot of fundamental questions not only in ferromagnetic thin films but also in very different systems such as atoms in superfluids and Bose–Einstein condensates and Cooper pairs in superconductors [6, 7]. On the other hand, vortices might be used as a building block for future magnetic storage devices. For instance, Van Waeyenberge *et al* very recently found a way to switch the vortex core with short magnetic field pulses [8], which was also investigated by theoretical approaches [9, 10]. Furthermore magnetic vortex cores are interacting with artificial defects and can be trapped by those, e.g. holes or antidots [11, 12]. If more than one such defect is created a switching between different vortex core trapped states, which might serve as discrete levels in a multivalent memory device, can be achieved [13]. The interaction between vortices and pinning sites in discs have also been investigated by Monte Carlo and analytical simulations [14, 15]. While the dynamic properties of vortices in circular discs and squares have been studied intensively by applying different techniques [5, 16–19], the magnetization dynamics of ferromagnetic discs in the presence of central holes has been probed by time-resolved scanning transmission x-ray microscopy and Kerr microscopy so far [20, 21]. However, almost all studies concerning vortex–hole or vortex–antidot interactions reported so far have been performed on circular permalloy discs, which comprise one (stray field

[4] Present address.

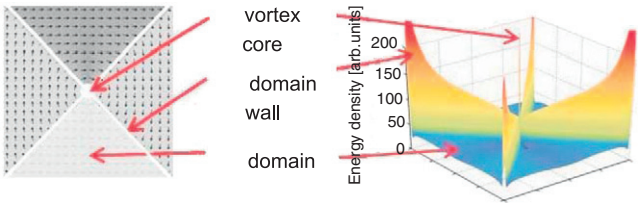

Figure 1. Left: simulated magnetization in a mesoscopic soft magnetic square showing a Landau-flux-closure pattern. Right: the energy density in the same mesoscopic square.

minimized) in-plane magnetization curl around the center of the disc, in which the out-of-plane vortex core is located. There are few works on the magnetization dynamics of a permalloy square comprising non-centric holes up to now [22, 23].

In comparison to a mono-domain disc a square exhibits four single domains, and stray field minimization is achieved via 90° domain walls, which are not present in circular discs. The vortex core, in the center of the Landau-flux-closure structure, is directly connected to the domain walls. Domain walls occur also in every multivortex structure, and thus are important for the dynamic properties of almost every (sub)-micrometer structure beyond simple vortex structures in circular discs or ellipses. Recently a very different dynamic behavior for two-vortex or vortex–antivortex–vortex configurations, depending on the individual core polarizations, has been found. These results may be attributed to the exchange interaction between the cores and the adjacent domain walls [24, 25].

Figure 1 shows the simulated energy densities of the three subunits of a Landau-flux-closure structure, namely the domains, the domain walls and the vortex core. The domains are the lowest energy region of the overall structure, whereas introduction of domain walls leads to an increase of the exchange energy, resulting in a higher energy density. The highest energy density is found for the vortex core region, which can be seen as a narrow spike in the center of figure 1 (right). It is clear that a defect should have quite a different influence on the magneto-static and magneto-dynamic behavior of the overall sample, dependent in which subunit it is introduced. Here we report on the influence of holes in domains, domain walls and the center on the overall magnetization dynamics of Landau-flux-closure structures. For this purpose we systematically prepared permalloy squares with central holes and a different number of non-centric holes either in the domain walls or the domains themselves. In order to tackle the spectrum of magnetic eigenexcitations we applied a stroboscopic pump probe technique using time-resolved photo-emission electron microscopy (PEEM). The experimental results are compared to micromagnetic simulations.

2. Experimental and simulation details

Permalloy ($Ni_{81}Fe_{19}$) squares of various orientations, between 3 and 6 μm width and 20 nm thickness, were prepared on a 10 μm wide coplanar waveguide. Holes of ≈100–200 nm diameter were drilled at different positions into the sample by means of focused ion beam (FIB) milling.

The time and spatially resolved magnetization was measured using the photo-emission electron microscope (PEEM) at the SIM beamline of the Swiss Light Source. The magnetic contrast was imaged applying x-ray magnetic circular dichroism (XMCD) at the Fe L_3 edge, where the image intensity is $I \propto M_y(\vec{r}) \cdot \vec{P}$. The experimental lateral resolution is around 50 nm. We use a grayscale representation, with white representing a parallel and black an antiparallel orientation of the magnetization to the x-ray polarization. The samples are excited every 16 ns using magnetic field pulses synchronized to the x-ray pulses emitted by the synchrotron. The time dependence is measured by varying the time delay Δt [18]. The field pulse $\vec{H}_p$ is along the y direction, has a magnitude of $\vec{H}_p \approx 30$ Oe and a temporal width of about 1 ns with a rise time of about 150 ps.

The micromagnetic simulations were carried out with a commercially available program package [26]. We use standard permalloy material parameters: exchange constant $A = 1.05 \times 10^{-11}$ J m^{-1}, saturation magnetization $M_s = 8 \times 10^5$ A m^{-1} and uniaxial anisotropy $K_u = 100$ J m^{-3}. As the corresponding experiments were performed at room temperature, thermal effects have been neglected for the simulations ($T = 0$ K). The static images were calculated assuming a strongly overestimated magnetic damping constant $\alpha = 1$ due to faster convergence, for all dynamic simulations $\alpha = 0.01$ was chosen. The amplitude (A), frequency (f) and damping (α_{GM}) values of the gyrotropic mode were derived by fitting the core position (x_{VC}, y_{VC}) with a damped harmonic oscillation: $[x_{VC}, y_{VC}] = A \exp(-\alpha_{GM} t) \sin(2\pi f t)$. Note that α_{GM} corresponds to the damping of the gyrotropic mode and not to the Gilbert damping α which is unaffected by modifications of the sample shape.

3. Results and discussion

3.1. Micromagnetic simulations of a number of different configurations

First we want to discuss the influence of defects on the vortex gyrotropic mode by means of micromagnetic simulations. Therefore we performed simulations on a series of samples comprising different numbers and types of voids at different positions. We focus on non-centric defects here, since the influence of a hole removing the vortex core itself has been studied intensely by previous works [11–14, 20, 27, 28]. Figure 2 displays a number of different configurations which we want to address in the following. Static simulations are considering a small external field of 25 Oe in order to displace the vortex, before instantly removing this field to excite the magnetization dynamics[5].

[5] In order to keep the computation times acceptable the simulations presented in section 3.3 have been performed on 1 μm squares and diameter discs of 20 nm thickness, respectively. In the magnetic ground state simulations a 25 Oe strong external field in the x direction has been applied to displace the vortex cores significantly from equilibrium positions. During the dynamic simulations this field was instantly removed, so that the vortex gyrates freely back into its magnetic equilibrium position. All other parameters were chosen as described in sections 2, 3.1 and 3.2.

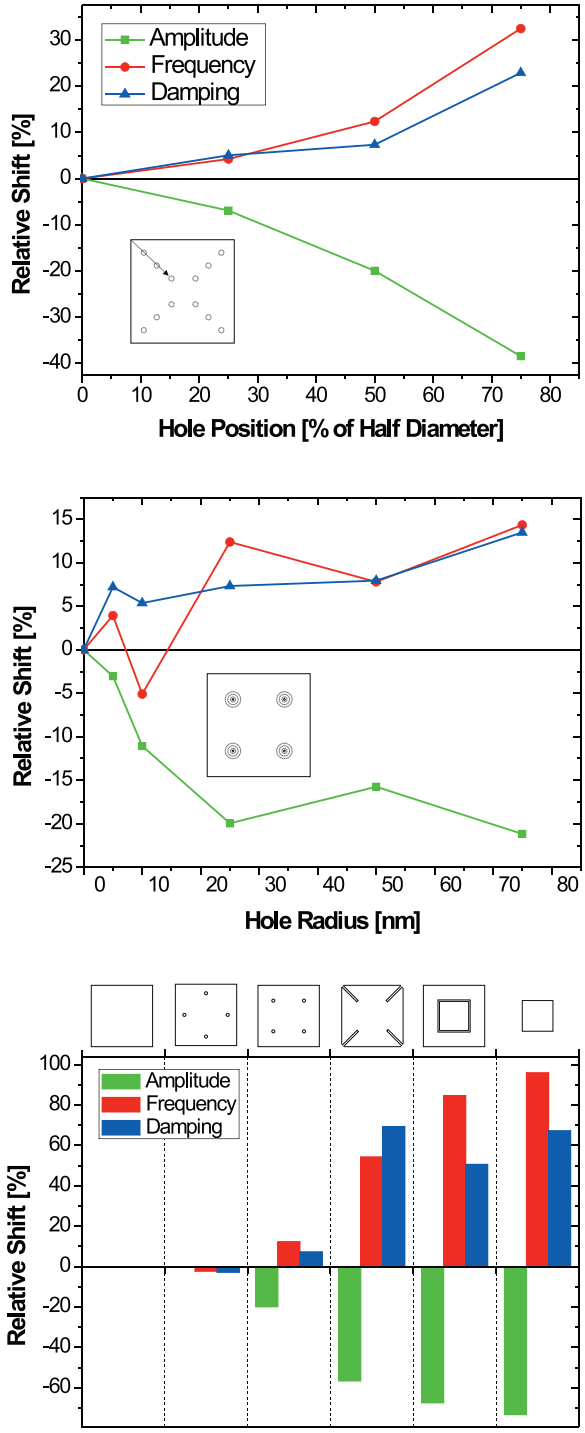

Figure 2. Results of micromagnetic simulations considering holes at different positions and sizes in a 1 μm $\times$ 1 μm permalloy square. Top: changes in amplitude (green), frequency (red) and damping (blue) of the vortex gyrotropic mode in dependence of the position of holes in the four domain walls. Center: dependence of the vortex gyrotropic mode varying due to the hole size places in the four domain walls. Bottom: dependence of the vortex gyrotropic mode on different kinds of defects placed in different positions of the permalloy square.

The top panel of figure 2 presents results of simulations considering permalloy squares comprising a hole of 25 nm diameter in each domain wall, placed in between each sample corner and the vortex core, leading to an overall amount of four such defects. The position of these defects is varied from 75% over 50% to 25% of the distance between the vortex core in magnetic equilibrium (center) and the sample corners. The corresponding diagram displays the results of the relative shifts of the frequency, damping and amplitude of the vortex gyrotropic mode as to a reference sample without defects (i.e. relative shifts = 0%). Holes placed into the domain walls lead to a significant higher frequency and damping, and to a lower amplitude of the vortex gyrotropic mode. If the holes are positioned at half the distance between the sample corners and the vortex core in magnetic equilibrium (sample center), the frequency of gyration is enhanced more than 10% whereas the damping is enhanced slightly less than 10%, resulting in an around 20% reduced amplitude of the vortex gyration. Recently, such results have also been found experimentally [22].

Also an increase of the hole size positioned in the domain walls has a significant influence on the properties of the gyrotropic mode (figure 2, center). Increasing the diameter of the holes leads to about 15% increased vortex frequency and damping, respectively. The amplitude is reduced $\sim$20% compared to a defect-free permalloy square. We want to mention that the curves in the middle panel are not monotonic, in contrast to the results shown in the top and bottom panels. It is unclear whether this is due to a numerical modeling variation or of physical origin.

Finally we want to discuss the influence of different defects on the properties of the vortex gyrotropic mode in mesoscopic permalloy squares (see bottom panel, figure 2). All kinds of defects investigated in this work tend to increase the frequency and the damping of the vortex gyrotropic mode. On the other hand, the amplitude of the gyration is lower compared to that of a defect-free reference sample. First we want to mention a significant difference of samples comprising hole-like defects either in the domains or the domain walls (second and third samples from the left in the bottom panel of figure 2). Whereas such defects, placed into the domain walls, have a relatively large influence on the properties of the vortex gyrotropic mode (as discussed before), almost no change of gyration is found in cases of equally large defects positioned in the magnetic domains. This can be explained by the fact that the high energy density components, like the domain wall and the vortex core, are stabilized by the gain in stray field energy E_d resulting from the flux-closure pattern. Since the domain wall and the vortex core have a high energy density they can be pinned to a certain point in the mesoscopic object if this region is made non-magnetic. If one cuts out complete parts of the domain walls (third sample from right) one observes an even stronger effect on the vortex gyrotropic mode. Cutting out a complete square part of the sample (second sample from right) leads to a gyrotropic mode that is already quite similar to that of a permalloy square of the size of the inner part (500 nm, first sample from right). However, some magneto-static and magneto-dynamic interactions between the outer frame and inner square are still present. On the other hand, the values for the defect-free squares of different sizes (1 μm, 500 nm) are in agreement with previously achieved results: $1/f \propto$ lateral size [29].

With these investigations from micromagnetic simulations we now want to discuss the results of experimental data of mesoscopic permalloy squares comprising artificial defects.

3.2. Landau-flux-closure structures with central holes

Focused ion beam milling (FIB) allows controlled introduction of such non-magnetic defects into thin film samples. For this a finely focused beam of high kinetic energy ions is directed onto the sample. By properly selecting the ion type and the kinetic energy one can either remove the magnetic thin film, creating a hole, or destroy the magnetism by ion-induced defects and doping [30, 31].

An example of defects created using FIB is shown in figure 3. In the scanning electron microscope (top) they show up as dark spots. Shown are two squares with a single defect at the center (configuration I) and the same defect at the center plus two defects along the diagonal (configuration II). These squares were imaged in the PEEM using the geometry shown schematically at the bottom. In the PEEM image the defects are not clearly visible. Their diameter is given by the region irradiated using the FIB. This needs to be of the order of the width of the vortex core or the domain wall ($\sim\xi$) to be an effective pinning site. Micromagnetic simulations show that, as expected, the changes of the magnetization produced by the defects are limited to a distance a few times the size of the defects. Because the size of the defects is close to the resolution of the PEEM, they are not clearly visible in the PEEM images. To show the effect of pinning on the dynamics we present a sequence of images of these defect-containing structures following the excitation by a field pulse $\mathbf{H_P}$.

Comparing the results shown for the defect containing squares in figure 4 with those of the defect-free squares [18] we observe clear differences. The defects pin the vortex core and thus hinder its motion. For defect-free squares the core and the domain walls move along the $-x$ direction. The small defect apparently pins the vortex for configuration I. In the difference images $M_y(\mathbf{r}, \Delta t) - M_y(\mathbf{r}, \Delta t = 0)$ the bulging of the walls in the $-x$ direction is still visible (as seen by the white line in the difference images). Comparing configurations I and II we see that at short delays ($t \leqslant 600$ ps) the domain wall moves visibly in both the upper and the lower half of the square. For long delays ($t \geqslant 900$ ps) the wall in the upper half is still displaced, while in the lower half it has already returned to the equilibrium position. Apparently the pinning site acts as a knot for the wall oscillation, thus increasing frequency and relaxation time. Further investigations (not shown) revealed that the pinning potential of the defects is higher for the vortex core than for the domain walls. The reason is that the energy density associated with the vortex core is much higher than that associated with the domain walls. The vortex core is also very narrow (diameter $\sim \xi \sim 10$ nm) and the energy gain when keeping it in the non-magnetic defect region is very high. Defects can thus be used to selectively influence the dynamics of the domain wall and of the vortex core. Depending on the size, number and position of such defects the dynamic response of mesoscopic magnetic objects can be tailored.

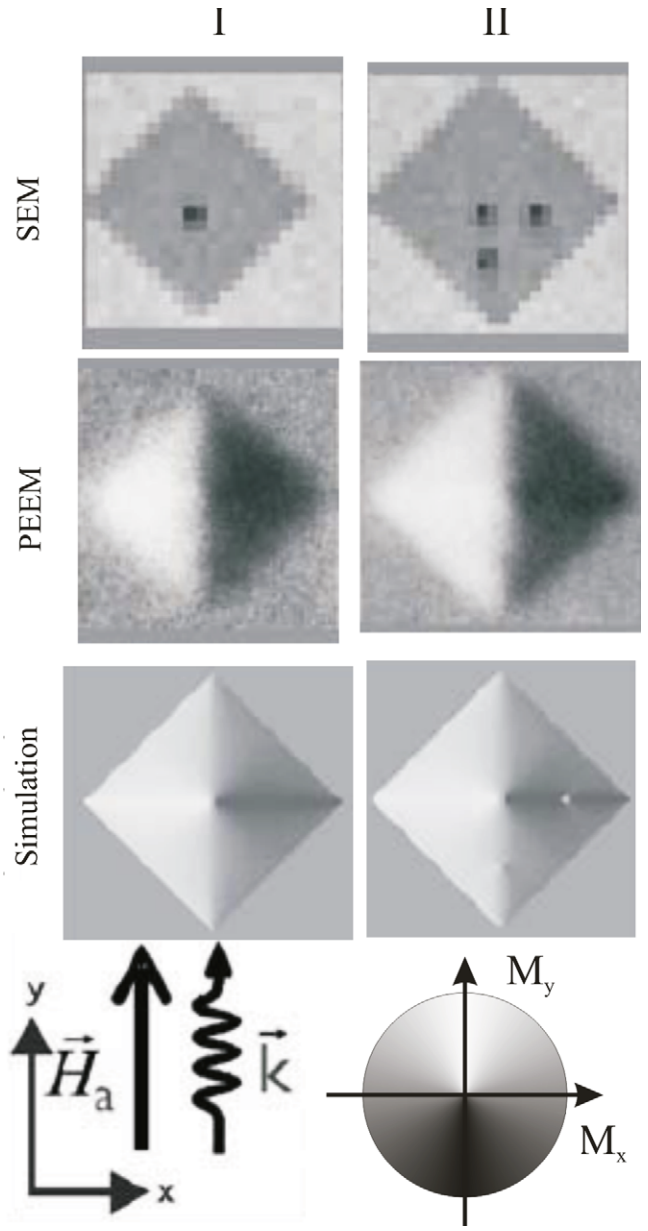

Figure 3. Defects in mesoscopic magnetic squares produced using a focused ion beam (FIB). The defects are clearly visible as dark spots in the scanning electron microscope (SEM) images (top). The PEEM images show the magnetic domain configuration (M_y contrast) of the same squares (middle). Here the defects are not well visible. The micromagnetic simulations (bottom) show that the defects cause a change of the magnetization only in a small region which is close to the resolution limit of the PEEM. Configuration I ($a = 3$ μm) contains a single defect pinning the vortex core, while in configuration II ($a = 4$ μm) two additional defects are pinning the domain walls.

3.3. Landau-flux-closure structure with non-centric holes

We now discuss the magnetization dynamics of samples III–V. The first 2 ns were imaged with a high density of data points ($\Delta t = 50$ ps) in order to investigate the domain and domain wall modes. Then a series over a full excitation cycle of 16 ns with less dense data points ($\Delta t = 500$ ps) was recorded in order to get more detailed information about the different vortex gyrations.

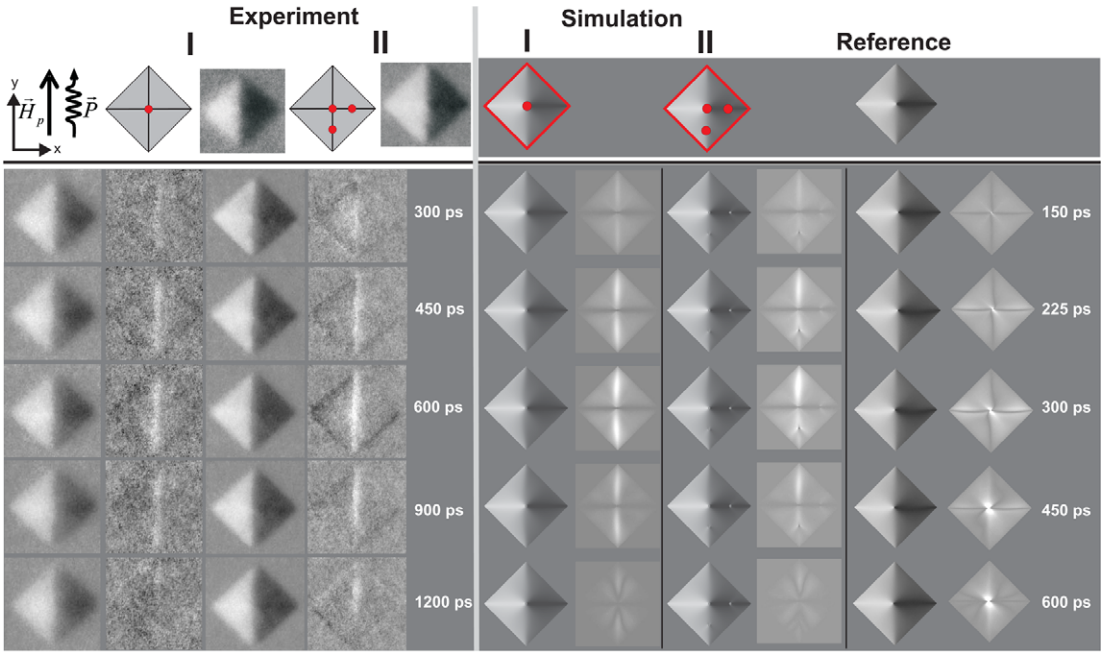

Figure 4. Dynamics of two magnetic squares, containing controlled defects, following excitation by a field pulse H_P. Experiments (left) can be compared to simulations (right). To increase the visibility of small changes caused by the field pulse we show difference images $M_y(r, \Delta t) - M_y(r, \Delta t = 0)$ adjacent to all images.

Figure 5 shows dynamic images and their subsequent difference images $M_y(\vec{r}, \Delta t) - M_y(\vec{r}, 0)$ at the indicated delay times. The experimental geometry is equivalent to that in section 3.3. 350 ps after the field pulse excitation the domains of all three samples show a dynamic response in the form of a magnetic excursion, in particular within the domains with a magnetization vector perpendicular to the exciting pulse. Thus these domains appear brighter in the magnetic contrast and the difference images at $\Delta t = 350$ ps and 750 ps, respectively. At $\Delta t = 750$ ps the region around the right hole of sample III also shows changing magnetic contrast. This indicates the dynamic vortex–hole interaction via the conjunctive domain wall. In sample V no interaction between the vortex or the domain walls and the holes in the left and right domains is observed throughout the experiment. Between 1 and 1.5 ns the domain walls show the most activity in samples III and IV whereas the walls of sample V are already close to equilibrium. All three samples show further domain wall activities at somewhat longer delay times (not shown here). The domain walls are bulging to the opposite side of their initial excitation, but with reduced amplitudes. The relatively coarse data point density of 0.5 ns at $\Delta t \geqslant 2$ ns does not resolve details. Coming back to the images taken at $\Delta t = 1000$ and 1500 ps, one can investigate how the domain walls are pinned by the holes at 1000 ps. At 1500 ps only the parts between vortex core and holes are active in sample III. In sample IV only the wall without holes can be seen in the difference image. At much longer delay times the magnetization dynamics is dominated by the regions around the vortex cores in each sample (see, e.g., the image at $\Delta t = 7500$ ps). Next we compare our experimental PEEM images with corresponding simulations (right panel of figure 5), again considering reduced sample dimensions by keeping the square length to sample thickness ratio constant[6]. Like in section 3.3 we find that the domain and domain wall motions are about twice as fast as in the experiment. However, at longer delays, i.e. the dynamics is dominated merely by the vortex gyrotropic mode, the agreement between the experimental and the simulated timescale is very good. This can be seen at the 7.5 ns image in figure 5. The good agreement of the vortex gyrotropic motion in simulation and experiment can be attributed to the fact that the excursion of the vortex core is very small, and hence sample boundaries play only a minor role.

3.4. Conclusions

In summary we studied the influence of small defects on the magnetization dynamics of mesoscopic permalloy squares comprising Landau-flux-closure structures. Simulations considering holes placed into the domain walls predict a significant influence on the vortex gyrotropic mode. In particular, the frequency and the damping are enhanced, whereas the amplitude of the vortex gyration is significantly reduced. Experiments on samples with point defects in the center of the sample, i.e. removing the vortex core and domain walls, demonstrate that such defects, introduced in parts of the samples showing a high energy density, can effectively pin these subunits, namely the vortex core and the domain walls, once the amplitude of the dynamic excitation is small enough. For domain walls this is also the case if no hole is introduced into the sample center and the dynamic response to a field pulse excitation is tuned by the defects pinning the wall. Simulations predict an enhanced frequency of the

[6] Static and dynamic simulations in section 3.2 were performed as described in section 3.1. However, to take into account resonant excitation we simulate three full 16 ns excitation cycles.

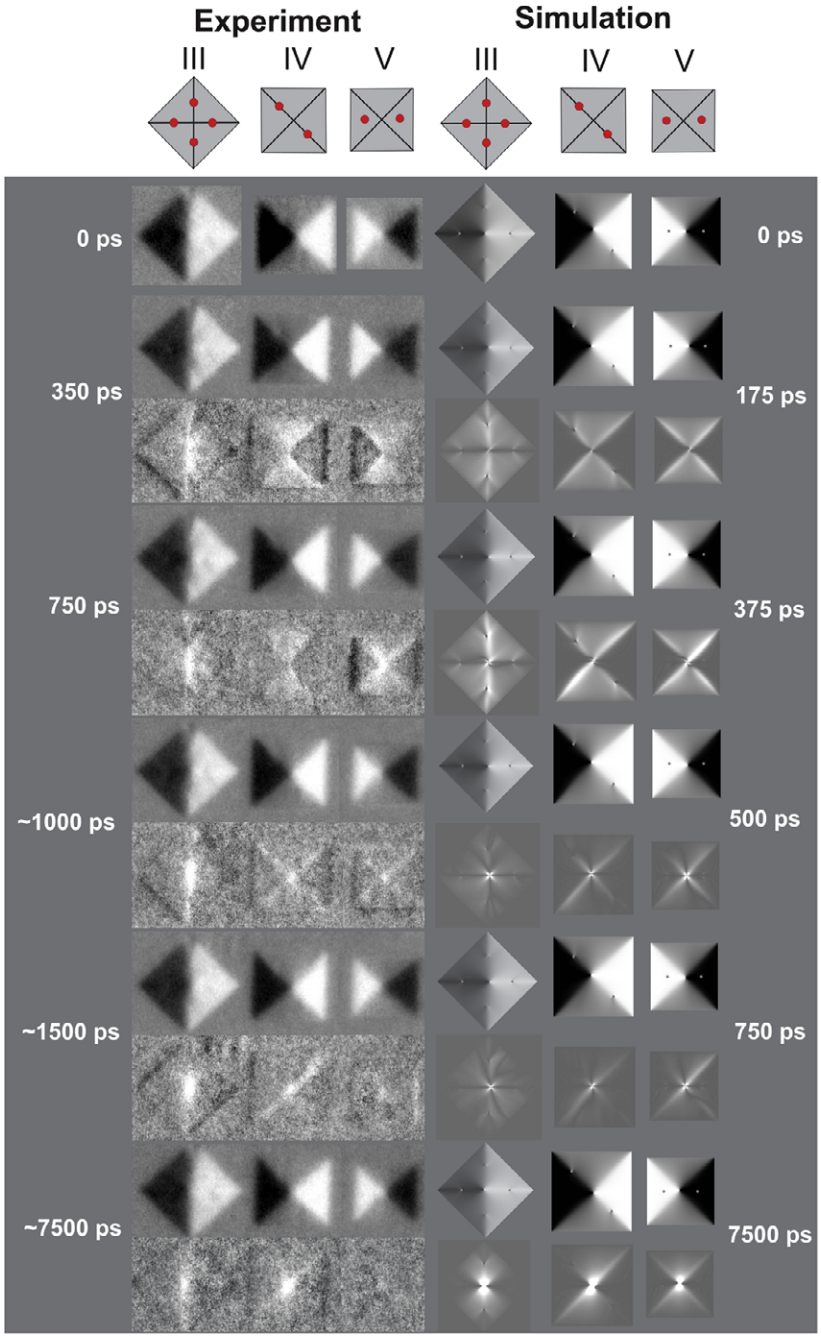

Figure 5. Magnetization $M_y(\vec{r}, \Delta t)$ of samples III–V at different characteristic delay times. The corresponding difference images $M_y(\vec{r}, \Delta t) - M_y(\vec{r}, 0)$ are shown below each original magnetic contrast image. Left panel: experimental data, right panel: corresponding simulations.

gyrotropic mode. In our experiments this effect is not visible, likely due to the limitations in temporal and lateral resolution. Depending on the size, number and position of artificial defects the dynamic response of mesoscopic permalloy squares can be tailored. This can be useful for generating bistable magnetic configurations which in principle can be used for data storage.

Acknowledgments

Part of this work has been performed at the Swiss Light Source, Paul Scherrer Institut, Villigen, Switzerland. We are indebted to D Weiss (University of Regensburg) for making the cleanroom available. KK and SW acknowledge travel support from the EU's Sixth Framework Programme.

References

[1] Hubert A and Schäfer R 1998 *Magnetic Domains* (Berlin: Springer)
[2] Shinjo T, Okuno T, Hassdorf R, Shigeto K and Ono T 2000 *Science* **289** 930
[3] Raabe J, Pulwey R, Sattler R, Schweinböck T, Zweck J and Weiss D 2000 *J. Appl. Phys.* **88** 4437

[4] Wachowiak A, Wiebe J, Bode M, Pietzsch O, Morgenstern M and Wiesendanger R 2002 *Science* **298** 577
[5] Choe S-B, Acremann Y, Scholl A, Bauer A, Doran A, Stöhr J and Padmore H A 2004 *Science* **304** 420
[6] Xu Z A, Ong N P, Wang Y, Kakeshita T and Uchida S 2000 *Nature* **406** 486
[7] Abo-Shaer J R, Raman C, Vogels J M and Ketterle W 2001 *Science* **292** 476
[8] van Waeyenberge B *et al* 2006 *Nature* **444** 461
[9] Hertel R, Gliga S, Fähnle M and Schneider C M 2007 *Phys. Rev. Lett.* **98** 117201
[10] Yamada K, Kasai S, Nakatani Y, Kobayashi K, Kohno H, Thiaville A and Ono T 2007 *Nat. Mater.* **6** 270
[11] Rahm M, Stahl J, Wegscheider W and Weiss D 2004 *Appl. Phys. Lett.* **85** 1553
[12] Uhlig T, Rahm M, Dietrich C, Höllinger R, Heumann M, Weiss D and Zweck J 2005 *Phys. Rev. Lett.* **95** 237205
[13] Rahm M, Höllinger R, Umansky V and Weiss D 2004 *J. Appl. Phys.* **95** 6708
[14] Pereira A R, Mól L A, Leonel S A, Coura P Z and Costa B V 2003 *Phys. Rev.* B **68** 132409
[15] Pereira A R, Moura A R, Moura-Melo W A, Carneiro D F, Leonel S A and Coura P Z 2007 *J. Appl. Phys.* **101** 034310
[16] Gerrits T, van den Berg H A M, Hohlfeld J, Bär L and Rasing T 2002 *Nature* **418** 509
[17] Park J P, Eames P, Engebretson D M, Berezovsky J and Crowell P A 2003 *Phys. Rev.* B **67** 020403
[18] Raabe J, Quitmann C, Back C H, Nolting F, Johnson S and Buehler C 2005 *Phys. Rev. Lett.* **94** 217204
[19] Krüger B, Drews A, Bolte M, Merkt U, Pfannkuche D and Meier G 2007 *Phys. Rev.* B **76** 224426
[20] Kuepper K *et al* 2007 *Appl. Phys. Lett.* **90** 062506
[21] Hoffmann F, Woltersdorf G, Perzlmaier K, Slavin A N, Tiberkevich V S, Bischof A, Weiss D and Back C H 2007 *Phys. Rev.* B **76** 014416
[22] Vansteenkiste A, de Baerdemaeker J, Chou K W, Stoll H, Curcic M, Tyliszczak T, Woltersdorf G, Back C H, Schütz G and Van Waeyenberge B 2008 *Phys. Rev.* B **77** 144420
[23] Silva R L, Pereira A R, Silva R C, Moura-Melo W A, Oliveira-Neto N M, Leonel S A and Coura P Z 2008 *Phys. Rev.* B **78** 054423
[24] Buchanan K S, Roy P E, Grimsditch M, Fradin F Y, Guslienko K Y, Bader S D and Novosad V 2005 *Nat. Phys.* **1** 172
[25] Kuepper K, Buess M, Raabe J, Quitmann C and Fassbender J 2007 *Phys. Rev. Lett.* **99** 167202
[26] http://llgmicro.home.mindspring.com
[27] Moura-Melo W A, Pereira A R, Silva R L and Oliveira-Neto N M 2008 *J. Appl. Phys.* **103** 124306
[28] Silva R L, Pereira A R and Moura-Melo W A 2009 *J. Appl. Phys.* **105** 014314
[29] Novosad V, Fradin F Y, Roy P E, Buchanan K S, Guslienko K Y and Bader S D 2005 *Phys. Rev.* B **72** 024455
[30] Fassbender J and McCord J 2008 *J. Magn. Magn. Mater.* **320** 579
[31] Fassbender J, Bischoff L, Mattheis R and Fischer P 2006 *J. Appl. Phys.* **99** 08G301